

# Propene/Ethene-[1-<sup>13</sup>C] Copolymerization as a Tool for Investigating Catalyst Regioselectivity. MgCl<sub>2</sub>/Internal Donor/TiCl<sub>4</sub>–External Donor/AlR<sub>3</sub> Systems

Vincenzo Busico,<sup>†</sup> John C. Chadwick,<sup>‡,§</sup> Roberta Cipullo,<sup>\*,†</sup> Sara Ronca,<sup>†</sup> and Giovanni Talarico<sup>†</sup>

Dipartimento di Chimica, Università di Napoli Federico II, Via Cintia, 80126 Naples, Italy, and Dutch Polymer Institute, Laboratory of Polymer Chemistry, Eindhoven University of Technology, P.O. Box 513, 5600 MB Eindhoven, The Netherlands

Received May 7, 2004; Revised Manuscript Received August 2, 2004

**ABSTRACT:** The propene/ethene-[1-<sup>13</sup>C] copolymerization method has been applied to measure precisely the regioselectivity of two modern MgCl<sub>2</sub>-supported Ziegler–Natta catalyst systems for the industrial production of isotactic polypropylene, namely MgCl<sub>2</sub>/di(isobutyl)-*o*-phthalate/TiCl<sub>4</sub>–cyclohexylmethyldimethoxysilane/AlR<sub>3</sub> (**1**) and MgCl<sub>2</sub>/2,2-di(isobutyl)-1,3-dimethoxypropane/TiCl<sub>4</sub>–AlR<sub>3</sub> (**2**). System **2** turned out to be slightly less regioselective than system **1** (on average, 0.26% 2,1 misinsertions instead of 0.18%), but the distribution of the regiodefects throughout the polymer was found to be more uniform, most likely as a result of a lower differentiation of the active species. This provides a simple explanation for the different response of the two catalysts to molecular hydrogen as a chain transfer agent. In system **1**, indeed, part of the active species are almost completely regioselective, which means that H<sub>2</sub> finds very few preferential “cutting points” in the form of growing chains with a sterically hindered 2,1 last-inserted unit; therefore, a higher H<sub>2</sub> partial pressure is needed—compared with system **2**—in order to achieve the same decrease of average polymer molecular mass.

## Introduction

In a previous paper,<sup>1</sup> we have reported on the application of the propene/ethene-[1-<sup>13</sup>C] copolymerization method<sup>2</sup> to measure the regioselectivity of MgCl<sub>2</sub>/TiCl<sub>4</sub>–AlR<sub>3</sub>, which can be viewed as the ancestor of all present-day MgCl<sub>2</sub>-supported Ziegler–Natta catalyst systems for the industrial production of isotactic polypropylene (iPP).<sup>3</sup>

As is well-known, TiCl<sub>4</sub> chemisorption on the coordinatively unsaturated side edges of MgCl<sub>2</sub> crystallites, followed by alkylation/reduction by AlR<sub>3</sub>, gives rise to a variety of active species differing profoundly in stereoselectivity.<sup>3–5</sup> In fact, polymer fractionation and <sup>13</sup>C NMR microstructural characterization reveal the copresence of highly isotactic, poorly isotactic (“isotactoid”) and predominantly syndiotactic polypropylene chains/stereoblocks.<sup>5</sup> In the <sup>13</sup>C NMR spectra of all fractions, on the other hand, regioirregular enchainments are hardly detectable, which has long been taken as an indication that, irrespective of the stereoselectivity, the regioselectivity of all active species in the quoted system (in favor of 1,2 insertion, as demonstrated by chain end group analysis) is very high.

Quite unexpectedly, we found instead that isolated 2,1 (secondary) insertions are relatively frequent (on average, 7 out of 1000, although broadly distributed throughout the polymer, in line with the multisite catalyst nature). This concentration is in principle well above the threshold for <sup>13</sup>C NMR observation; however, the fine structure of the resonances of isolated ethene-[1-<sup>13</sup>C] units in between propene units with opposite enchainments, used as markers of the regiodefects,

revealed that the 2,1 units are largely stereoirregular, also when they occur in highly isotactic polypropylene chain segments (Chart 1).<sup>1</sup>

Obviously, the resonances of the head-to-head/tail-to-tail enchainments in the propene homosequences are similarly split and broad, which explains why their detection is problematic for polymer samples at natural <sup>13</sup>C abundance. As a matter of fact, a 15% enrichment in <sup>13</sup>C at the methyl C was necessary to reveal, in the spectrum of a propene homopolymer, the methyl peaks of the two sequences of Chart 2 with a signal-to-noise ratio allowing a reliable integration.

Consistently with the indications obtained from the microstructural analysis of the copolymers, the said two sequences were found to occur in comparable amounts also in the “isotactic” (i.e., boiling-heptane-insoluble) fraction. This has important implications on the nature of the active species, as we shall see in the following.

A large body of experimental and theoretical evidence supports the hypothesis that TiCl<sub>n</sub> deposition on MgCl<sub>2</sub> surface is epitaxial.<sup>3–5</sup> Three basic structures can be envisaged for the active species (Figure 1, A–C), depending on the specific side edge of MgCl<sub>2</sub> carrying them (i.e., 100-like or 110-like) and on the possible proximity to a “defective” surface location (such as, e.g., a corner, a step, etc.).

It has long been recognized by computer modeling that these structures result in dramatically different stereoselectivities. In particular, molecular mechanics (MM) calculations by Corradini and co-workers<sup>6</sup> demonstrated that propene enantiodiscrimination requires the presence of a surface Cl atom (in black in Figure 1) which reduces the conformational freedom of the growing polymer chain at S1 or S2, forcing the first C–C bond to assume a chiral orientation. This, in turn, favors 1,2 monomer insertion at the other site with the enantioface directing the methyl group anti to the said

<sup>†</sup> Università di Napoli Federico II.

<sup>‡</sup> Eindhoven University of Technology.

<sup>§</sup> On secondment from Basell Polyolefins.

\* Corresponding author. E-mail: cipullo@chemistry.unina.it.

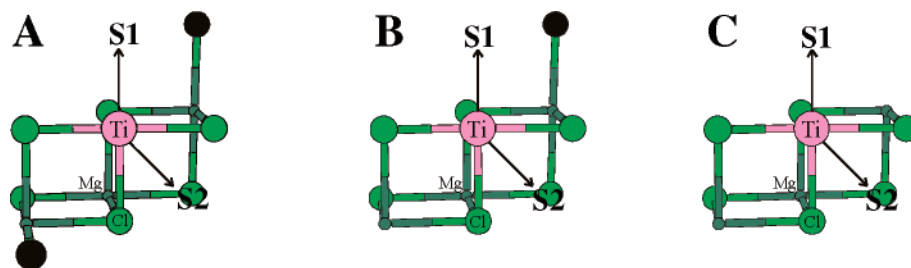
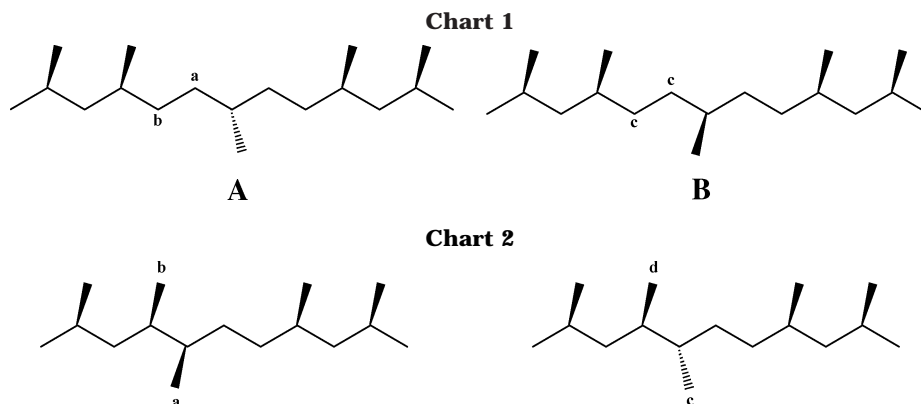


**Figure 1.** Models of active Ti species on the surface of  $\text{MgCl}_2$  in donor-free systems (see text).



C–C bond (Figure 2). The MM conclusions are fully consistent with experimental results by Zambelli and co-workers.<sup>7</sup>

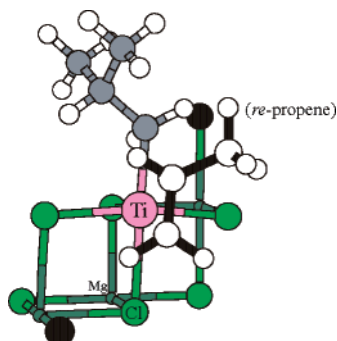


**Figure 2.** Optimized geometry corresponding to the transition state for the favored (*re* enantioface) 1,2 propene insertion at the  $C_2$ -symmetric model species **A** of Figure 1 ( $\Delta$  configuration; growing chain simulated with an isobutyl group).

In view of the above, it is straightforward to conclude<sup>5</sup> that the two homotopic sites S1 and S2 of species **A** are enantioselective, whereas one of the two diastereotopic sites of species **B** (namely, S1), and both homotopic sites of species **C**, are not. As a result, chain propagation can be predicted to be tout-court isotactic at **A**; atactic at **C** (unless chain-end control is operative); hemiisotactic, atactic, or isotactic at **B**, depending on whether monomer insertion takes place with regular chain migration or preferentially at S1 or at S2, respectively.

Recent calculations with full quantum mechanics (QM) methods<sup>1</sup> have substantially confirmed the MM ones, although—not unexpectedly—the latter seem to have overestimated, in general, site enantioselectivities.

New experimental results are also consistent with the said picture. Homogeneous  $C_2$ -symmetric Zr-based catalysts with stereorigid tetradentate [ONNO] ligands mimicking species **A** and **C** of Figure 1 turned out to produce enantiomorphous-site-controlled isotactic and chain-end-controlled predominantly syndiotactic polypro-

pylene, respectively.<sup>8</sup> On the other hand, thorough high-field  $^{13}\text{C}$  NMR microstructural characterizations of polypropylene samples obtained with a number of  $\text{MgCl}_2$ -supported catalyst systems, including  $\text{MgCl}_2/\text{TiCl}_4\text{--AlR}_3$ , gave evidence for “isotactoid” sequences with a configurational statistics clearly reminiscent of hemiisotactic polypropylene and as such traceable to  $C_1$ -symmetric active species like, e.g., **B** in Figure 1.<sup>5,9</sup>

Concerning the regioselectivity, full QM calculations on propene insertion at model species **A** pointed out<sup>1</sup> a moderate preference for 1,2 insertion, with a  $\Delta E^\ddagger$  value of ca. 2 kcal/mol, in very reasonable agreement with the experiment. However, 2,1 insertion was predicted to be highly enantioselective in favor of the enantioface orienting the methyl group anti to the nearest Cl atom colored in black in Figure 1 (see details in Figure 3, left);

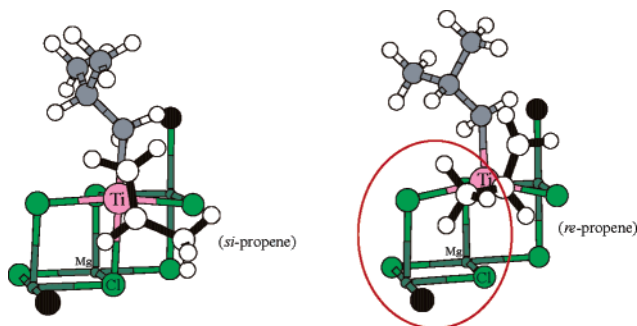


**Figure 3.** Optimized geometries of the transition states for the favored (*si* enantioface, left) and disfavored (*re* enantioface, right) 2,1 propene insertion at the  $C_2$ -symmetric model species **A** of Figure 1 ( $\Delta$  configuration; growing chain simulated with an isobutyl group).

insertion with the opposite enantioface instead appears to be practically prohibited due to the strong repulsive interaction between the two moieties (Figure 3, right). To reconcile the latter result with the experimental fact that the 2,1 units are stereoirregular also in the “isotactic” polypropylene fraction (Chart 2), one needs to admit that most 2,1 insertions occur at active species

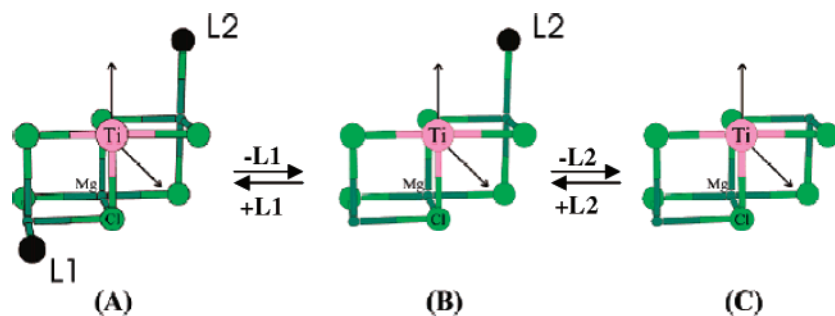


**Figure 4.** General three-site dynamic model of active species for  $\text{MgCl}_2$ -supported Ziegler-Natta catalysts (see text and ref 9b). L1 and L2 = Cl,  $\text{AlR}_x\text{Cl}_{3-x}$ , or Lewis base.

in which at least one of the said Cl atoms is missing (e.g., **B** of Figure 1) and that such species are capable of generating highly isotactic sequences/chains or—more plausibly—that they are in equilibrium with species **A**, which would temporarily lose a Cl atom and thus generate poorly regular blocks in otherwise highly isotactic chains.

Independent experimental evidence of a stereoblock chain nature, implying a fluxional behavior of the active species (Figure 4), was provided by the cited high-field <sup>13</sup>C NMR microstructural analyses<sup>5,9</sup> and—more recently—by thorough polymer fractionation and crystallization studies.<sup>10</sup>

Atom mobility at the surface of metal and ionic lattices, in general, is a known fact. In the specific case of  $\text{MgCl}_2/\text{TiCl}_4\text{--AlR}_3$ , the additional hypothesis can be made that mobile Cl atoms come from molecules of  $\text{AlR}_2\text{--Cl}$  (generated from the  $\text{AlR}_3$  cocatalyst at the alkylation step), which adsorb reversibly on the surface.<sup>9b,11</sup>

Relative to  $\text{MgCl}_2/\text{TiCl}_4\text{--AlR}_3$ , industrial catalyst systems for iPP production differ mainly in that they contain suitable Lewis bases, added as “internal donor” (ID) components of the solid catalyst or as “external donor” (ED) together with the cocatalyst  $\text{AlR}_3$ .<sup>3–5</sup> As is well-known, donor modification results in a tremendous increase of stereoselectivity; the “isotactic” fraction (conventionally defined as the part of the polymer which is not extracted by boiling heptane or recrystallizes in xylene at room temperature after hot dissolution) is typically greater than 95 wt %, and more typically greater than 97%, whereas in the absence of donors it amounts to less than 50%.

Although the mechanisms of catalyst modification by Lewis bases are not fully clarified, there is compelling experimental evidence that the presence of donor molecules affects the stereoselectivity in a way that points to their presence at nonbonded contact with the active species. In particular, not only the weight amount of the “isotactic” polymer fraction but also its degree of stereoregularity is higher after donor addition.<sup>12</sup> An easy way to account for these observations is to admit that, in the equilibrium of Figure 4, L1 and L2 are not necessarily Cl atoms but can also be donor molecules. Strongly coordinating donors would shift the equilibrium to the left, which would explain the observed increase in “isotactic” fraction content; at the same time, a higher enantioselectivity of the active sites is to be expected when L1 or L2 is a bulky organic molecule rather than Cl.<sup>5,9b</sup>

How Lewis bases affect catalyst regioselectivity is less known and is the subject of this paper. In particular, the propene/ethene-[1-<sup>13</sup>C] copolymerization approach has been applied to two modern industrial systems,

namely  $\text{MgCl}_2/\text{di}(\text{isobutyl})\text{--}o\text{-phthalate}/\text{TiCl}_4\text{--cyclohexylmethylmethoxysilane}/\text{AlR}_3$ <sup>13</sup> and  $\text{MgCl}_2/2,2\text{-di}(\text{isobutyl})\text{-1,3-dimethoxypropane}/\text{TiCl}_4\text{--AlR}_3$ ,<sup>14</sup> (from here on, systems **1** and **2**, respectively) to quantify the frequency and the stereochemistry of 2,1 propene insertion. Moreover, the fundamental issue of the relationship between catalyst regioselectivity and hydrogen response has been addressed.

### Experimental Section

The two catalysts  $\text{MgCl}_2/\text{di}(\text{isobutyl})\text{--}o\text{-phthalate}/\text{TiCl}_4$  and  $\text{MgCl}_2/2,2\text{-di}(\text{isobutyl})\text{-1,3-dimethoxypropane}/\text{TiCl}_4$  were prepared according to literature procedures.<sup>13,14</sup>  $\text{Al}(\text{isobutyl})_3$  was used as the cocatalyst because  $\text{AlEt}_3$  (which is the elective choice in industrial practice) is known to undergo  $\beta\text{-H}$  elimination and liberate ethene, which in our case would contaminate the copolymers.

All propene/ethene-[1-<sup>13</sup>C] copolymerizations were run in a 100 mL jacketed Pyrex reactor, equipped with a magnetic stirrer, a silicone rubber septum, and a gas inlet/outlet, according to the following procedure. The reactor was charged under nitrogen with 50 mL of dry heptane (Aldrich) containing 0.15–0.22 mL of  $\text{Al}(\text{isobutyl})_3$  (Crompton) and, for catalyst system **2**, 0.0167 mL of cyclohexylmethylmethoxysilane. The reactor was thermostated at 50 °C, and a gaseous mixture of propene (SON, Polymerization Grade) and ethene-[1-<sup>13</sup>C] (Isotec Inc.; 99.9% isotopic purity) at the appropriate composition, prepared with vacuum-line techniques and standardized by gas chromatography, was bubbled through the liquid phase at atmospheric pressure and a flow rate of 0.09 L/min, until gas/liquid equilibrium was attained. The reaction was then started by injecting through the serum cap the catalyst (5–15 mg), previously suspended in 5.0 mL of dry heptane, and allowed to proceed for 10–30 min, during which the comonomer mixture was kept flowing through the liquid phase at the said rate. Under such conditions, total monomer conversion was lower than 20%, which ensured a nearly constant comonomer feeding ratio. After quenching the reaction with 5 mL of methanol/HCl(aq,conc) (95/5 v/v), the copolymer was coagulated with excess methanol/HCl, filtered, washed with more methanol, and vacuum-dried.

The list of all copolymers prepared is given in Table 1. To separate the “isotactic” from a “less tactic” fraction, all copolymers were subjected to exhaustive Kumagawa extraction with a convenient boiling solvent, chosen in such a way that the weight amount of the insoluble fraction and the <sup>13</sup>C NMR degree of stereoregularity of the propene homosequences contained in it (normalized  $[\text{mmmm}] > 93\%$ ) were similar to the corresponding parameters for the reference propene homopolymer (see again Table 1). The comparatively high solubility in boiling heptane (20 wt %) of the homopolymer prepared with catalyst **2** reflects the increase in the proportion of the weakly tactic polymer fraction when the polymerization is carried out in the absence of hydrogen.<sup>15</sup>

Quantitative <sup>13</sup>C NMR spectra of the copolymers were recorded with a Varian VXR 200 spectrometer operating at 50.3 MHz on 100 mg/mL solutions in tetrachloroethane-1,2-

**Table 1. List of the Propene/Ethene-[1-<sup>13</sup>C] Copolymers Prepared with Catalyst Systems 1 and 2 and Results of Their Fractionation with a Convenient Boiling Solvent (See Text)**

catalyst system	sample no.	[E]/[P] × 10 <sup>3</sup> (liquid phase) <sup>a</sup>	Q <sub>E</sub> (mol %)	extracting solvent	"isotactic" fraction (wt %) <sup>b</sup>
<b>1</b>	EP1	0.46	0.40 (1)	hexane	94.3
	EP2	1.1	1.13 (2)	pentane	95.5
	EP3	1.5	1.72 (2)	diethyl ether	92.7
	EP4	2.0	2.73 (2)	diethyl ether	92.0
	EP5	5.0	5.80 (5)	diethyl ether	90
<b>2</b>	EP6	0.57	0.67 (1)	hexane	81
	EP7	1.42	1.74 (2)	pentane	71
	EP8	4.2	3.20 (5)	diethyl ether	69
	EP9	5.9	6.00 (5)	diethyl ether	65

<sup>a</sup> E = ethene-[1-<sup>13</sup>C], P = propene. <sup>b</sup> Values of I.I. (extraction with boiling heptane) for the corresponding propene homopolymers: 96% for **1**, 80% for **2**.

**Table 2. <sup>13</sup>C NMR Mole Fraction of Ethene-[1-<sup>13</sup>C] Units Following a 2,1 Propene Unit (Q<sub>SE</sub>) as a Function of Total Ethene-[1-<sup>13</sup>C] Content (Q<sub>E</sub>) for Propene/Ethene-[1-<sup>13</sup>C] Copolymers Prepared with Catalyst Systems 1 and 2**

catalyst system	sample no.	Q <sub>E</sub> (mol %)	Q <sub>SE</sub> (mol %)
<b>1</b>	EP1	0.40 (1)	0.014 (2)
	EP2	1.13 (2)	0.035 (2)
	EP3	1.72 (2)	0.042 (3)
	EP4	2.73 (2)	0.057 (3)
	EP5	5.80 (5)	0.092 (5)
<b>2</b>	EP6	0.67 (1)	0.052 (3)
	EP7	1.74 (2)	0.12 (1)
	EP8	3.20 (5)	0.15 (1)
	EP9	6.00 (5)	0.18 (1)

d<sub>2</sub> at 120 °C. Conditions: 5 mm probe; 76° pulse; acquisition time, 2.0 s; relaxation delay, 1.5 s; 30K–60K transients. The spectra were fully simulated with the Shape2004 software package.<sup>16</sup>

## Results and Discussion

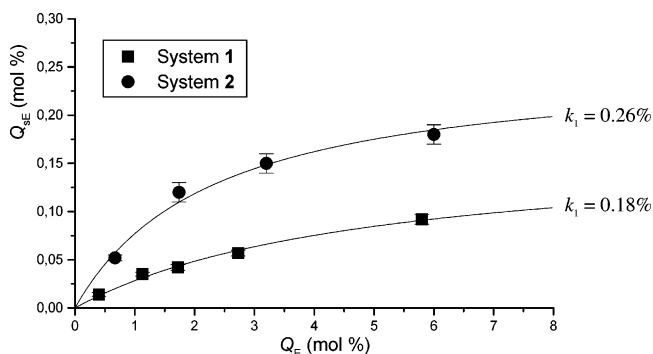
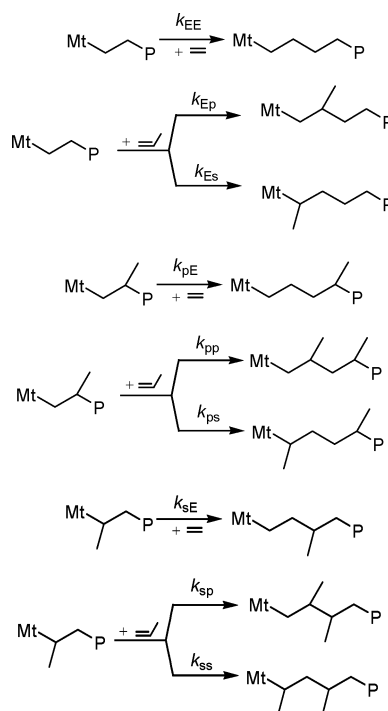
In Table 2, we report, for all propene/ethene-[1-<sup>13</sup>C] copolymers prepared with catalyst systems **1** and **2**, the mole fraction of ethene-[1-<sup>13</sup>C] units found by <sup>13</sup>C NMR to be adjacent to a 2,1 (secondary) propene unit (Q<sub>SE</sub>) as a function of total ethene-[1-<sup>13</sup>C] incorporation (Q<sub>E</sub>).

Plots of Q<sub>SE</sub> vs Q<sub>E</sub> (Figure 5) show the expected<sup>1,2</sup> asymptotic behavior, well-fitted by a simple saturation function:

$$Q_{SE} = k_1 Q_E / (k_2 + Q_E) \quad (1)$$

with the upper limit  $k_1$  being the fraction of 2,1 insertions in propene homopolymerization, i.e., the ratio of kinetic constants  $k_{ps}/k_{pp}$  in Scheme 1 (P = polymeryl).

Compared with the donor-free MgCl<sub>2</sub>/TiCl<sub>4</sub>-Al(isobutyl)<sub>3</sub> system, for which we had measured<sup>1</sup>  $k_1 = 0.72$  mol %, both **1** and **2** are much more regioselective ( $k_1(\mathbf{1}) = 0.18$  mol %,  $k_1(\mathbf{2}) = 0.26$  mol %). On the other hand, it is important to realize that also for such systems the above are only *average* values and that the distribution of the 2,1 units throughout the polymer is not uniform. In this respect, the <sup>13</sup>C NMR characterization of the "isotactic" copolymer fractions (Table 3 and Figure 6) revealed an important difference between **1** and **2**: for the former, the 2,1 unit content of the "isotactic" fraction is *really* low ( $k_1(\mathbf{1-iso}) = 0.078$  mol %), which implies that most regiodefects (ca. 1.0 mol %) are concentrated in the "less tactic" fraction; in the latter, instead, the difference in the degree of regioregularity of the two fractions is less extreme (0.15 mol % vs 0.5 mol %),

**Figure 5.** Mole fraction of ethene-[1-<sup>13</sup>C] units adjacent to a 2,1 propene unit (Q<sub>SE</sub>) vs total ethene-[1-<sup>13</sup>C] content (Q<sub>E</sub>) for propene/ethene-[1-<sup>13</sup>C] copolymers prepared with systems **1** and **2** (best-fit curves in accordance with eq 1).**Scheme 1****Table 3. <sup>13</sup>C NMR Mole Fraction of Ethene-[1-<sup>13</sup>C] Units Following a 2,1 Propene Unit (Q<sub>SE</sub>) as a Function of Total Ethene-[1-<sup>13</sup>C] Content (Q<sub>E</sub>) for the "Isotactic" Fraction of Propene/Ethene-[1-<sup>13</sup>C] Copolymers Prepared with Catalyst Systems 1 and 2**

catalyst system	sample no.	Q <sub>E</sub> (mol %)	Q <sub>SE</sub> (mol %)
<b>1</b>	EP1	0.37 (1)	0.0125 (15)
	EP2	1.00 (2)	0.022 (2)
	EP3	1.56 (2)	0.033 (2)
	EP4	2.20 (3)	0.036 (3)
	EP5	3.60 (4)	0.048 (3)
<b>2</b>	EP6	0.54 (2)	0.015 (2)
	EP7	1.34 (2)	0.027 (2)
	EP8	2.40 (3)	0.046 (2)
	EP9	4.70 (5)	0.069 (3)

which represents a further indication that the active species of 1,3-diether-containing catalysts<sup>14</sup> are less differentiated than those of diester-modified ones.<sup>13</sup>

Another important point to be made is that, at odds with the case of the donor-free catalyst system, for which—as we have already noted in the Introduction—both sequences **A** and **B** of Chart 1 are detected in the <sup>13</sup>C NMR spectra of the propene/ethene-[1-<sup>13</sup>C] copolymers, in comparable amounts even in the "isotactic"

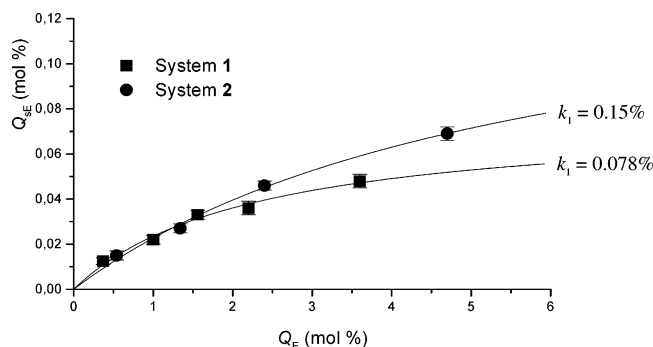


**Figure 6.** Mole fraction of ethene-[1-<sup>13</sup>C] units adjacent to a 2,1 propene unit ( $Q_{\text{adj}}$ ) vs total ethene-[1-<sup>13</sup>C] content ( $Q_E$ ) for the “isotactic” fractions of propene/ethene-[1-<sup>13</sup>C] copolymers prepared with systems **1** and **2** (best-fit curves in accordance with eq 1).

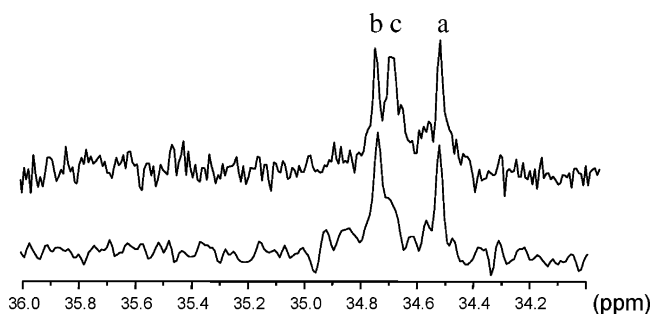


**Figure 7.** Details of the  $S_{\alpha\beta}$  region of the <sup>13</sup>C NMR spectrum of a propene/ethene-[1-<sup>13</sup>C] copolymer prepared with system **1** (sample EP4 of Table 1, lower trace) and, for comparison, of the “isotactic” fraction of a similar copolymer prepared with system  $\text{MgCl}_2/\text{TiCl}_4\text{--Al(isobutyl)}_3$  (upper trace). The chemical shift scale is in ppm downfield of TMS. The assignment<sup>1</sup> refers to Chart 1.

fraction (Figure 7, top), in the spectra of copolymers obtained with **1** and **2** (Figure 7, bottom) sequence **A** is largely predominant. This proves that 2,1 insertion at the active species of such systems is substantially enantioselective and—in very nice agreement with the predictions of QM modeling<sup>1</sup> for model species **A** of Figures 1 and 4—in favor of the enantioface which is instead less reactive in 1,2 insertion (Figures 2 and 3).

The above picture is consistent with the hypothesis<sup>5,9b</sup> that the addition of strongly coordinating donors shifts the equilibrium of Figure 4 to the left. Moreover, the substantial increase of regioselectivity relative to the donor-free case is also an indication that, in the active species conforming to model **A**, ligands L1 and/or L2 are bulkier than Cl atoms. As a matter of fact, the space-filling representation of species **A** (Figure 8) shows that, already when  $L1 = L2 = \text{Cl}$ , the methyl group of a 2,1-inserting propene unit is at close nonbonded contact with either L1 or L2. Therefore, it is easy to predict that any further increase of steric hindrance leads to a decrease in the reactivity of 2,1 propene even with the favored enantioface.

Another important issue to be addressed is catalyst “dormancy” consequent to the regioirregular insertions. We<sup>17</sup> and others<sup>18</sup> reported experimental results suggesting that the reactivity toward propene of a growing polypropylene chain is (much) lower when the last-inserted unit is 2,1 (rather than 1,2). Somewhat counterintuitively, the possible accumulation of these “dormant” chains is *not* dependent on the frequency of 2,1 insertion (i.e., on the ratio  $k_{\text{ps}}/k_{\text{pp}}$ ) but only on the ratio of specific rates  $k_{\text{sp}}/k_{\text{ps}}$  (definitions in Scheme 1). At



**Figure 8.** Space-filling representation of the transition state structure of Figure 3, left.

stationary state, and in the hypothesis of negligible chain transfer, it can be demonstrated<sup>2,17</sup> that the fraction of dormant sites,  $x_d^*$ , is given by

$$x_d^* = (1 + k_{\text{sp}}/k_{\text{ps}})^{-1}$$

Just as an example, this corresponds to  $x_d^* = 50\%$  for  $k_{\text{sp}}/k_{\text{ps}} = 1$  and to  $x_d^* = 90\%$  for  $k_{\text{sp}}/k_{\text{ps}} = 0.1$ . In other words, the apparent specific rate of polymerization,  $\langle k_p \rangle$ , in the said two cases would be 50% and 10% of  $k_{\text{pp}}$ , respectively. Therefore, it is easy to understand that the 2,1 units, even when present in trace amounts, can produce a major “bottleneck” in the kinetics of polymerization.

The reactivity of dormant sites can be substantially higher with molecules smaller than propene. In particular, the much higher insertion rate of ethene vs propene into  $\text{M--CH}(\text{CH}_3)\text{--CH}_2\text{--P}$  forms the basis for the propene/ethene-[1-<sup>13</sup>C] copolymerization method itself.<sup>2</sup> Much more relevant from the technological standpoint, though, is the reactivity with  $\text{H}_2$ , which is used as a molecular mass regulator in industrial iPP production.<sup>3</sup> Convincing evidence has accumulated that the small  $\text{H}_2$  molecule is not slowed down when reacting with secondary  $\text{M--polymeryl}$  bonds and that, therefore in the competition with propene, hydrogen is highly favored for reactivity with dormant chains.<sup>17,18</sup> This has two important consequences: (i) last-inserted 2,1 units are preferential chain cutting points by  $\text{H}_2$ ; (ii)  $\text{H}_2$  can have an activating effect on the polymerization.<sup>19</sup>

Not all catalysts, however, respond to  $\text{H}_2$  in the same way. In particular, it has been observed that, *coeteris paribus*,  $\text{MgCl}_2$ -supported systems modified with a dialkyl phthalate as ID and an alkoxysilane as ED (e.g., system **1**) require a higher  $\text{H}_2$  pressure to achieve a given polypropylene average molecular mass than systems containing a 1,3-diether as ID (e.g., system **2**); it is common to read that the “hydrogen response” of the latter systems is higher.<sup>15</sup> A simple explanation for this now comes from our measurements of regioselectivity. As we have seen before, in the polymer produced with **1** the 2,1 units are mostly concentrated in the “less tactic” fraction, which represents less than 10 wt %; the “isotactic” fraction, instead, contains less than 1 regioirregular enchainment out of 1000, which means that the preferential “cutting” points for  $\text{H}_2$  along the chains are very few. Conversely, in the polymer obtained with **2** the distribution of the 2,1 units is narrower, and even the most stereoregular fraction contains almost two regioirregular enchainments out of 1000; therefore,  $\text{H}_2$  finds more points of preferential attack. How this

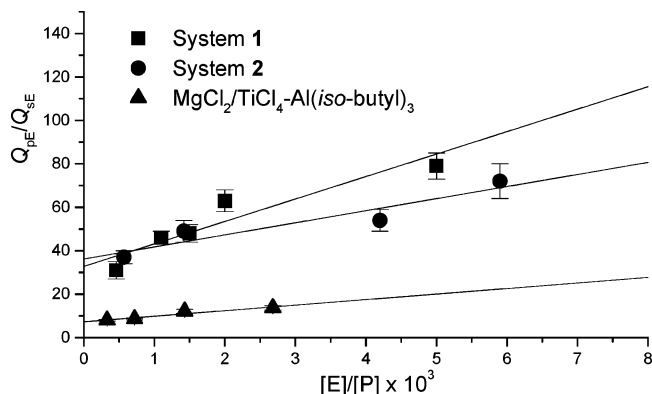


**Figure 9.** Ratio of ethene-[1-<sup>13</sup>C] units following a 1,2 or a 2,1 propene unit ( $Q_{pE}/Q_{sE}$ ) vs ethene/propene feeding mole ratio in the liquid phase ( $[E]/[P]$ ) for the "isotactic" fractions of propene/ethene-[1-<sup>13</sup>C] copolymer samples prepared with different catalyst systems (data from Tables 1 and 3 and ref 1).

influences polymer rheological and crystallization behavior will be the subject of a subsequent independent paper.<sup>20</sup>

Measuring and comparing catalyst dormancy, on the other hand, is more complicated because that would require knowledge of  $k_{sp}/k_{ps}$ . In previous papers,<sup>1,2,17</sup> we have noted that this ratio can be determined experimentally only as an aggregated product with another ratio of specific rates. In particular, making use of propene/ethene-[1-<sup>13</sup>C] copolymerization data,<sup>2</sup> one can plot the ratio  $Q_{pE}/Q_{sE}$  ( $Q_{pE} = Q_E - Q_{sE}$ ) as a function of the ethene/propene feeding ratio and obtain a straight line which intercepts the ordinate axis at  $(Q_{pE}/Q_{sE})_0 = (k_{sp}/k_{ps})(k_{pE}/k_{sE})$  (for the definition of all kinetic constants, refer, as usual, to Scheme 1).

Figure 9 shows the said plot for the "isotactic" fractions of copolymers prepared with systems **1** and **2** (data taken from Tables 1 and 3) and also, for comparison, with  $MgCl_2/TiCl_4-Al(isobutyl)_3$ .<sup>1</sup> Because of the multisite nature of all three systems, even when referring to the quoted fraction, one needs to keep in mind that the extrapolated values of  $(k_{sp}/k_{ps})(k_{pE}/k_{sE})$  are averages over a whole family of catalytic species. This being said, it is remarkable that, for the two donor-containing, highly stereoselective systems,  $(k_{sp}/k_{ps})(k_{pE}/k_{sE})$  is similar and much higher than for the donor-free one. In our opinion, this should be traced to the fact that, in the former systems, even ethene "feels" the steric difference between a primary and a secondary M–polymeryl bond and inserts more slowly in the latter bond ( $k_{pE}/k_{sE} > 1$ ). This is in line with a higher steric congestion of an active species like, e.g., **A** of Figure 4 when L1 and L2 are bulky donor molecules rather than Cl atoms. A similar tendency of  $k_{pE}/k_{sE}$  to increase with increasing site enantioselectivity has recently been reported for single-center metallocene catalysts as well.<sup>21</sup>

Unfortunately, the above suggests that the simplifying assumption, plausible for poorly stereoselective systems, that in the product  $(k_{sp}/k_{ps})(k_{pE}/k_{sE})$  the ratio  $k_{pE}/k_{sE}$  is close to unity is untenable for **1** and **2**; this precludes the possibility to disaggregate  $k_{sp}/k_{ps}$ .

Results of chain end group analysis for polypropylene samples prepared in the presence of catalyst systems (similar to) **1** and **2** at variable H<sub>2</sub> pressure indicate that, in the limit of  $p(H_2) \rightarrow 0$ , the fraction of *n*-butyl ends generated by hydrogenolysis of dormant chains is

substantially higher in the latter case, which points to a correspondingly higher value of  $x_d^*$  (or, equivalently, to a lower value of  $k_{sp}/k_{ps}$ ).<sup>13c</sup> With these systems, catalyst productivity in the presence of hydrogen is typically a factor 3–5 higher than is observed in the absence of hydrogen.<sup>15,22</sup> This hydrogen activation effect appears to be greatest for the diether-containing catalyst **2**, in line with the higher proportion of *n*-butyl-terminated chains, but it should also be taken into account that in the case of ester-containing systems the overall activating effect of hydrogen may be limited by partial catalyst deactivation resulting from reaction of the ester with Ti–H bonds formed in chain transfer with hydrogen.<sup>23</sup>

## Conclusions

In this paper, the propene/ethene-[1-<sup>13</sup>C] copolymerization method has been applied to measure precisely the regioselectivity of two modern  $MgCl_2$ -supported Ziegler–Natta catalyst systems for the industrial production of isotactic polypropylene, namely  $MgCl_2/di(isobutyl)-o-phthalate/TiCl_4$ -cyclohexylmethyldimethoxysilane/ $AlR_3$  (**1**) and  $MgCl_2/2,2-di(isobutyl)-1,3-dimethoxypropane/TiCl_4-AlR_3$  (**2**). The results demonstrate that system **2**, which is slightly less regioselective than system **1** (on average, 0.26% 2,1 misinsertions instead of 0.18%), distributes the regiodefects throughout the polymer more uniformly, most likely as a result of a more uniform nature of the active species. This explains the different hydrogen response of the two catalysts; in system **1**, in fact, part of the active species are almost completely regioselective, which means that H<sub>2</sub> finds very few preferential "cutting points" (i.e., 2,1 last-inserted units) in the growing chains, and therefore a higher H<sub>2</sub> partial pressure is needed—compared with system **2**—in order to achieve the same decrease of average polymer molecular mass. The implications of the latter finding on the rheological and crystallization behavior of the polymer will be the subject of a forthcoming paper.<sup>20</sup>

**Acknowledgment.** Financial support from the Italian Ministry for Education (PRIN 2002) is acknowledged.

## References and Notes

- (1) Busico, V.; Cipullo, R.; Polzone, C.; Talarico, G.; Chadwick, J. C. *Macromolecules* **2003**, *36*, 2616–2622.
- (2) (a) Busico, V.; Cipullo, R.; Ronca, S. *Macromolecules* **2002**, *35*, 1537–1542. (b) Busico, V.; Cipullo, R.; Talarico, G.; Caporaso, L. *Macromolecules* **1998**, *31*, 2387 and reference 12 therein.
- (3) Moore, E. P. J. *Polypropylene Handbook: Polymerization, Characterization, Properties, Applications*; Hanser Publishers: Munich, 1996; Chapter 2.
- (4) Corradini, P.; Busico, V.; Guerra, G. *Comprehensive Polymer Science*; Pergamon Press: Oxford, UK, 1988; Vol. 4, pp 29–50.
- (5) Busico, V.; Cipullo, R. *Prog. Polym. Sci.* **2001**, *26*, 443–533.
- (6) (a) Corradini, P.; Barone, V.; Fusco, R.; Guerra, G. *J. Catal.* **1982**, *77*, 32–42. (b) Corradini, P.; Barone, V.; Fusco, R.; Guerra, G. *Gazz. Chim. Ital.* **1983**, *113*, 601–607. (c) Corradini, P.; Busico, V.; Cavallo, L.; Guerra, G.; Vacatello, M.; Venditto, V. *J. Mol. Catal.* **1992**, *74*, 433–442. (d) Monaco, G.; Toto, M.; Guerra, G.; Corradini, P.; Cavallo, L. *Macromolecules* **2000**, *33*, 8953–8962.
- (7) (a) Zambelli, A.; Locatelli, P.; Sacchi, M. C.; Rigamonti, E. *Macromolecules* **1980**, *13*, 798–800. (b) Zambelli, A.; Amendola, P. *Prog. Polym. Sci.* **1991**, *16*, 203–218.

- (8) Busico, V.; Cipullo, R.; Ronca, S.; Budzelaar, P. H. M. *Macromol. Rapid Commun.* **2001**, *22*, 1405–1410.
- (9) (a) Busico, V.; Cipullo, R.; Talarico, G.; Segre, A. L.; Chadwick, J. C. *Macromolecules* **1997**, *30*, 4786–4790. (b) Busico, V.; Cipullo, R.; Monaco, G.; Talarico, G.; Vacatello, M.; Chadwick, J. C.; Segre, A. L.; Sudmeijer, O. *Macromolecules* **1999**, *32*, 4173–4182.
- (10) Alamo, R. G.; Blanco, J. A.; Agarwal, P. K.; Randall, J. C. *Macromolecules* **2003**, *36*, 1559–1571.
- (11) Liu, B.; Nitta, K.; Nakatani, H.; Terano, M. *Macromol. Chem. Phys.* **2002**, *203*, 2412–2421 and references therein.
- (12) Morini, G.; Albizzati, E.; Balbontin, G.; Mingozzi, I.; Sacchi, M. C.; Forlini, F.; Tritto, I. *Macromolecules* **1996**, *29*, 5770–5776.
- (13) (a) Parodi, S.; Nocchi, R.; Giannini, U.; Barbè, P. C.; Scatà, U. EP 45977, 1982; *Chem. Abstr.* **1982**, *96*, 181808v. (b) Collina, G.; Morini, G.; Ferrara, G. *Polym. Bull. (Berlin)* **1995**, *35*, 115–120. (c) Chadwick, J. C. *Macromol. Symp.* **2001**, *173*, 21–35.
- (14) (a) Albizzati, E.; Giannini, U.; Morini, G.; Galimberti, M.; Barino, L.; Scordamaglia, R. *Macromol. Symp.* **1995**, *89*, 73–89. (b) Albizzati, E.; Barbè, P. C.; Noristi, L.; Scordamaglia, R.; Barino, L.; Giannini, U.; Morini, G. EP 361494, 1990; *Chem. Abstr.* **1990**, *113*, 153260.
- (15) Chadwick, J. C.; Morini, G.; Albizzati, E.; Balbontin, G.; Mingozzi, I.; Cristofori, A.; Sudmeijer, O.; Van Kessel, G. M. M. *Macromol. Chem. Phys.* **1996**, *197*, 2501–2510.
- (16) Shape2004, by Michele Vacatello, University of Naples Federico II.
- (17) (a) Busico, V.; Cipullo, R.; Corradini, P. *Makromol. Chem.* **1993**, *194*, 1079–1093. (b) Busico, V.; Cipullo, R.; Chadwick, J. C.; Modder, J. F.; Sudmeijer, O. *Macromolecules* **1994**, *27*, 7538–7543.
- (18) Tsutsui, T.; Kashiwa, N.; Mizuno, A. *Makromol. Chem., Rapid Commun.* **1990**, *11*, 565–570.
- (19) Guastalla, G.; Giannini, G. *Makromol. Chem., Rapid Commun.* **1983**, *4*, 519–527.
- (20) Chadwick, J. C.; van der Burgt, F. P. T. J.; Rastogi, S.; Busico, V.; Cipullo, R.; Talarico, G.; Heere, J. J. R. *Macromolecules*, to be submitted.
- (21) Borrelli, M.; Busico, V.; Cipullo, R.; Ronca, S.; Budzelaar, P. H. M. *Macromolecules* **2003**, *36*, 8171–8177.
- (22) Chadwick, J. C.; Van Kessel, G. M. M.; Sudmeijer, O. *Macromol. Chem. Phys.* **1995**, *196*, 1431–1437.
- (23) Albizzati, E.; Galimberti, M.; Giannini, U.; Morini, G. *Makromol. Chem., Macromol. Symp.* **1991**, *48/49*, 223–238.

MA049104A